6118–6131 *Nucleic Acids Research, 2008, Vol. 36, No. 19* *Published online 27 September 2008*
doi:10.1093/nar/gkn623

Human SWI/SNF directs sequence-specific chromatin changes on promoter polynucleosomes

Hillel I. Sims, Cassandra B. Baughman and Gavin R. Schnitzler*

Department of Biochemistry, Tufts University School of Medicine, Boston, MA 02111, USA

Received July 30, 2008; Revised September 9, 2008; Accepted September 11, 2008

ABSTRACT

Studies in humans and other species have revealed that a surprisingly large fraction of nucleosomes adopt specific positions on promoters, and that these positions appear to be determined by nucleosome positioning DNA sequences (NPSs). Recent studies by our lab, using minicircles containing only one nucleosome, indicated that the human SWI/SNF complex (hSWI/SNF) prefers to relocate nucleosomes away from NPSs. We now make use of novel mapping techniques to examine the hSWI/SNF sequence preference for nucleosome movement in the context of polynucleosomal chromatin, where adjacent nucleosomes can limit movement and where hSWI/SNF forms altered dinucleosomal structures. Using two NPS templates (5S rDNA and 601) and two hSWI/SNF target promoter templates (c-myc and UGT1A1), we observed hSWI/SNF-driven depletion of normal mononucleosomes from almost all positions that were strongly favored by assembly. In some cases, these mononucleosomes were moved to hSWI/SNF-preferred sequences. In the majority of other cases, one repositioned mononucleosome appeared to combine with an unmoved mononucleosome forming a specifically localized altered or normal dinucleosome. These effects result in dramatic, template-specific changes in nucleosomal distribution. Taken together, these studies indicate hSWI/SNF is likely to activate or repress transcription of its target genes by generating promoter sequence-specific changes in chromatin configuration.

INTRODUCTION

The fundamental unit of chromatin is the nucleosome, composed of 146 bp of DNA wrapped around an octamer of H2A, H2B, H3 and H4 core histone proteins. Nucleosomes impose a significant barrier to transcription by blocking access of activators and basal transcription factors to their DNA binding sites, as well as by inhibiting the elongation of engaged polymerase molecules (1). Since the linker DNA between nucleosomes, which averages ~60 bp in length, is far more accessible than nucleosome bound DNA, the precise location of nucleosomes on DNA can functionally control transcription factor binding. For instance, one recent study showed that removal of a repressive nucleosome was fully sufficient to drive Pol II recruitment and transcription on the yeast RNR3 promoter (2). Strikingly, recent studies have indicated that ~80% of all yeast nucleosomes adopt specific positions, and that these positions are often dictated by ~146 bp 'nucleosome positioning DNA sequences' (NPSs) that can be predicted from the primary DNA sequence (3–10). Within the last year, several other genome-wide studies have shown that positioned nucleosomes are also common in a variety of organisms from *Caenorhabditis elegans* to man (9,11–13, and for review see 14). These studies also showed that functional transcription factor binding sites, which are evolutionarily conserved or known to be bound *in vivo*, are much more frequently found in linker regions than in DNA covered by nucleosomes, and that start sites of active genes are frequently devoid of nucleosomes (4–6,12,15). This suggests that promoter DNA sequences regulate transcription, at least in part, through specific arrangements of evolutionarily selected NPSs relative to transcription factor binding sites. Overall, these observations indicate that the DNA sequence-directed positioning of nucleosomes is much more important for transcriptional regulation than was initially suspected, and emphasize the need for a deeper understanding of how nucleosome positions are functionally controlled.

One means by which all eukaryotic cells regulate the repressive effects of chromatin is the action of ATP-dependent chromatin remodeling complexes, which use the energy of ATP hydrolysis to modify chromatin structure. There are several conserved subfamilies of remodelers, each with distinct functions in transcriptional regulation and other nuclear processes. These include SWI/SNF, ISWI, CHD/NuRD, Ino80, Swr1, Rad54, CSB and DDM1 (for review see 16–19). Mammalian SWI/SNF complexes are tumor suppressors that are also

*To whom correspondence should be addressed. Tel: +1 617 636 2441; Fax: +1 617 636 2409; Email: gavin.schnitzler@tufts.edu

essential for embryonic development, heart development, heat shock, variable, diversity and joining (VDJ) recombination and the proper differentiation of hematopoetic, neuronal, myeloid and adipose cells (18). We are studying human SWI/SNF (hSWI/SNF), which functions as a transcriptional coactivator for a large number of human transcription factors (including all tested nuclear hormone receptors, MyoD, C-EBPβ, EKLF, NeuroD, c-myc and p53), and as a transcriptional corepressor through pRb, REST, MeCP2 and others (for review see 18–21).

All tested remodeling complexes have the ability to alter nucleosome positions on DNA, suggesting that nucleosome repositioning is a central aspect of remodeling complex function (16,17). Given that recent studies have shown a high fraction of nucleosomes are positioned *in vivo*, it is essential to understand the combined effects of DNA sequence and remodeling complexes on nucleosome positions. Studies by our lab and others, using linear mononucleosomes, attempted to address whether repositioning was controlled by underlying DNA sequences (22–28). While some hints of specificity were seen (e.g. 22,27,28), all of these studies were complicated by a strong tendency of hSWI/SNF [and related yeast remodels the structure of chromatin (RSC)] to move nucleosomes to DNA ends. We recently completed novel studies that measured the sequence preference of repositioning in the absence of DNA end effects, using small circular templates (minicircles) containing a single nucleosome (29). These studies showed that hSWI/SNF moved histone octamers away from assembly favored NPSs on two human c-myc promoter templates as well as one 5S rDNA NPS template, and placed them over a few complex-preferred sequences. This was the first demonstration, in the absence of DNA end effects, that any remodeling complex has an intrinsic sequence preference for repositioning. Together with recent studies indicating that a large fraction of nucleosomes are located over NPSs *in vivo*, these observations suggested that hSWI/SNF will activate or repress the transcription of specific promoters, at least in part, by moving nucleosomes away from default NPS-specified locations.

In other recent studies, we discovered that hSWI/SNF remodeling converts up to 40% of nucleosomes on polynucleosomal templates into novel structurally altered dinucleosomes, which we have named 'altosomes' [for 'altered dinucleosomes', (30)]. These structures appear to contain two intact histone octamers and protect a similar total amount of DNA from MNase digestion. However, instead of the single ~292 bp protected fragment typical of two closely abutting nucleosomes (a 'normal dinucleosome'), altosomes protect one internucleosomal sized fragment of ~220 bp, and one subnucleosomal fragment of ~70 bp. Also, while a normal dinucleosome will constrain two negative supercoils, the DNA wrapping around an altosome results in an abnormally low number of negative supercoils. The precise structure of the altosome is unknown, but will almost certainly contain ~220 bp region of DNA in tight association with both histone octamers, a bridge or loop of accessible DNA, followed by ~70 bp stretch of DNA bound tightly to histones. Possible functional roles for altosomes *in vivo* are suggested by studies showing that both reduced negative supercoiling and subnucleosomal MNase footprint products are associated with transcription, and can result from hSWI/SNF action (see citations in 30). In addition to altosomes, hSWI/SNF action can also increase the fraction of normal nucleosomes that lack linker DNA between them, generating dinucleosomes and higher multimers (30). Taken together, these studies suggest that the overall accessibility of hSWI/SNF-remodeled promoter chromatin will be determined by sequence-directed placement of all major hSWI/SNF products: mononucleosomes, altosomes and dinucleosomes.

Since our prior minicircle studies were limited to a single nucleosome, it was not possible to study how the underlying DNA sequence affects the formation and positioning of altosomes or dinucleosomes. In addition, while the complete freedom of mononucleosome movement allowed by the minicircle facilitated studies of hSWI/SNF sequence preference, it did not show how hSWI/SNF would reposition nucleosomes in the context of chromatin, where movement is restricted by the presence of surrounding nucleosomes. To answer these questions, we have now used a novel mapping approach to examine the effects of hSWI/SNF remodeling on the locations and abundance of mononucleosomes, altosomes and dinucleosomes, using four polynucleosomal templates, containing two well-characterized NPS sequences (*Xenopus* 5S rDNA and 601) and two known or suspected hSWI/SNF regulated gene promoter sequences (c-myc and UGT1A1). The results from these studies show that hSWI/SNF moves mononucleosomes away from strong NPSs and places mononucleosomes, altosomes and dinucleosomes on complex-preferred positions. They indicate that hSWI/SNF action can be differentially controlled by promoter DNA sequence and can result in dramatic changes in DNA accessibility. These sequence-directed remodeling effects provide new insights into the mechanisms by which hSWI/SNF activates or represses genes involved in cell growth and differentiation, and also into general mechanisms of transcriptional control by chromatin remodeling.

MATERIALS AND METHODS

Circular polynucleosomal arrays

The 5S template is the pXP10 plasmid, which contains a 241 bp region of the *Xenopus borealis* somatic 5S rDNA gene (31). A 2475-bp region from the c-myc promoter was PCR amplified from human MCF7 cell genomic DNA using the primers TCTCCTCTTCTTTGATCAG AATCGATGCAT and GACGTGGGTCTCTAGAGG TGTTAG, and subcloned into the Promega 11 ZF vector. The region extends from nucleosome 7 to 18 as mapped previously *in vivo* (32,33). The UGT1A1 promoter sequence in the pcDNA3.1 vector backbone was a kind gift of Dr Michael Court, TUSM, Pharmacology. The promoter sequence is from –873 bp to +118 bp relative to the transcriptional start site. The p601 plasmid contains the strong, artificial '601' NPS (34). Nucleosomes were assembled onto 20 μg of circular, supercoiled plasmid DNA by salt dilution using a 1.5:1 weight ratio of

human HeLa cell core histones to DNA, essentially as described in (30,35). The level of assembly was estimated to be one nucleosome per ~200 bp of DNA, based on topoisomerase I relaxation of chromatin followed by agarose gel electrophoresis of the purified DNA in the presence or absence of chloroquine (30).

Creation of probes for Southern hybridization

The 5S rDNA probe was PCR amplified from pXP10, using the primers GGGGGAAGCTTGTGGAATTGT GAGCGGATAACAATTTCACACAGG and AACCT TATGTATCATACACATAC. The product was digested with HindIII, generating a 359-bp fragment encompassing the 5S positioning sequence. The c-myc promoter probe sequences were PCR amplified using T7 and SP6 primers from our c-myc P1 and c-myc P1/P2 plasmids used previously to generate c-myc minicircle templates (29). The probes were digested with EcoRI to generate 359-bp fragments with 179 bp of overlapping sequence. The UGT1A1 probe was PCR amplified from the UGT1A1 plasmid using primers TGTTCACTCAAGAATGTGATTTGAG TATGAAATTCCAGCC and CGGGCCCTCTAGACT CGAGCGGC to generate a fragment from −227 to +173 relative to the UGT1A1 transcription start site. The 359-bp 601 probe was PCR amplified from p601 using the primers GGGGAAGCTTGTAATACGACT CACTATAGGGC and GGTGACACTATAGAATACT CAAGC. Approximately 80 ng of each probe was random hexamer labeled using αP^{32} dATP.

SWI/SNF remodeling, MNase digestion and nucleosomal species separation

hSWI/SNF was purified from HeLa Ini1 cells by immunoaffinity chromatography against the FLAG-tagged Ini1 subunit and stored in BC100 buffer (36). In general, four 30 µl reactions were arranged each with 190 ng of plasmid chromatin and 1.21 µg of hSWI/SNF (an hSWI/SNF to nucleosome ratio of ~0.4:1) in a buffer of 0.4 µg/µl BSA, 60 mM KCl, 0.55 mM ATP, 2.5 mM $MgCl_2$ and 0.1 units/µl wheat germ topoisomerase I (Promega, Madison, WI, USA). Control reactions were identical, except that BC100 buffer alone was used in place of hSWI/SNF. The reactions were incubated at 30°C for 2.5 h, and hSWI/SNF remodeling was stopped by the addition of ADP to a concentration of 10 mM. These conditions were previously found to allow the repositioning reaction to near completion after only 10 min on mononucleosome templates, and to result in an effective equilibrium of nucleosome positions that are most favored by hSWI/SNF by the 2.5 h time point (22,29). In initial tests, remodeling of p601 plasmid chromatin under these conditions was stopped at increasing times with apyrase, and the accessibility at the PmlI restriction site in the center of the 601 NPS measured. This assay showed that the hSWI/SNF-dependent increase in PmlI accessibility was 65% complete by 5 min and 76% complete by 20 min (consistent with the mapping results shown in Figure 2, data not shown). Lastly, we have previously shown that these conditions were sufficient to promote near maximal formation of altosomes after ~15 min of remodeling (30). For MNase digestion reactions, the buffer in each tube was adjusted to 1 mM $MgCl_2$, 3 mM $CaCl_2$, 65 mM KCl, 0.4 µg/µl BSA, 0.067 mM ATP and 2 mM ADP in a total volume of 150 µl. The reactions were prewarmed for several minutes at 30°C, digested with 0.4 unit/µl micrococcal nuclease (MNase, Roche, Basel, Switzerland, unit definition) for 5 min, and stopped by adjusting the buffer to 0.2% SDS and 15 mM EDTA. Note that the 20-fold molar excess of ADP over ATP in the MNase digestion buffer prevents any remodeling by hSWI/SNF during MNase treatment. MNase products were phenol extracted, ethanol precipitated in the presence of 50 µg of glycogen carrier and separated by 4% PAGE. Approximately146 bp mononucleosomal, ~290 bp dinucleosomal and ~220 bp altosomal products were separately excised, eluted by continuous shaking at 37°C in 2 to 3 gel volumes of TE overnight, and concentrated, where necessary, using a 10 kDa Millipore centrifugal filter.

Restriction enzyme digestion, Southern blotting and hybridization

For each restriction enzyme, an equal volume of eluted mononucleosomal, altosomal or dinucleosomal DNA was digested for 4 h in 20 µl reactions under supplier-specified ideal reaction conditions and using 10–20 U of each enzyme. The enzymes used for mapping were as follows: 5S (Figure 1D); c-myc—ScaI, MseI, HinfI, SmaI, BstYI, AvaII, ApaI, XhoI, Hpy188I and SfcI; UGT1A1—BamHI, ApoI, Hpy188I, HpyCHIV, ClaI, KasI, TseI, PstI, XbaI and MluI; 601—EcoRI, XbaI, PmlI, BsiWI, NotI, AvaII, PstI and HindIII. Note that, since any region of overlap between a nucleosomal fragment and the probe will result in some signal, restriction enzymes were chosen to be unique to both the probe region and 290 bp to either side (the length of a dinucleosome). Restriction digested samples were separated by 8% PAGE, along with 80 pg of unlabeled bare probe DNA fragments digested with each enzyme (to serve as both digestion controls and size markers). All gels were run for 550 Volt-hours. Following PAGE separation, the DNA was transferred to a positively charged nylon membrane by liquid transfer in 0.5× TBE at a constant 550 mA for 2.5 h. The membrane was denatured using 0.4 mM NaOH, renatured using 2× SSC and fixed to the membrane by UV cross-linking. Hybridization was done at 60°C, using the template-specific probes listed above. After hybridization, membranes were washed and exposed to a PhosphorImager screen, and visualized and quantitated using ImageQuant software (GE Healthcare Life Sciences, USA). Unlike our previous minicircle studies that used body labeling of the template to detect cut products, the application of Southern blotting allows us to map positions for a specific probe region within a >3-kb plasmid.

Analysis of mononucleosome, altosome and dinucleosome positions

Analysis of positions was done using novel modifications of our mononucleosome minicircle mapping procedure (29). Band lengths for each restriction digestion lane of

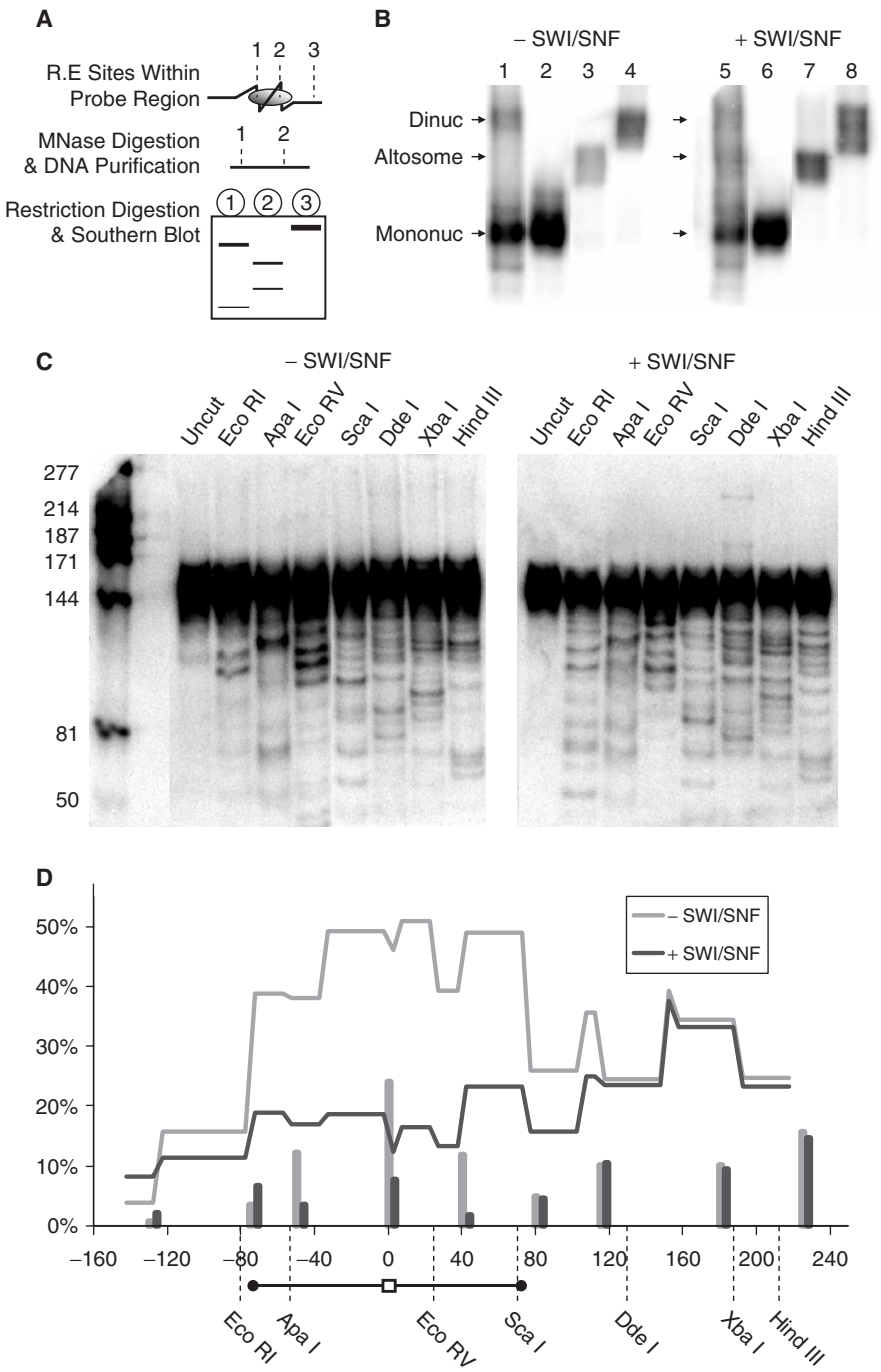

Figure 1. hSWI/SNF moves mononucleosomes away from the 5S positioning sequence on a polynucleosomal template. (**A**) Flow chart of mapping procedure, using the hypothetical case of a single, positioned mononucleosome in the probe region. Numbers and circled numbers denote restriction sites and restriction enzymes. (**B**) MNase-digested products from control and hSWI/SNF-remodeled 5S polynucleosome (lanes 1 and 5), the isolated ~146-bp mononucleosome (lanes 2 and 6), ~220-bp altosome (lanes 3 and 7) and ~292-bp dinucleosome (lanes 4 and 8) fragments were separated by PAGE and Southern blotted with the 5S NPS region probe. (**C**) Southern blot of restriction enzyme digestion products for the 146-bp MNase mononucleosome fragments with and without (+or−) SWI/SNF remodeling. (**D**) Bar graph representing percent occupancy (*y*-axis) and base pair position (*x*-axis) of midpoints for all mapped mononucleosomes, from control (gray) and remodeled (black) templates. Lines represent the summed mononucleosome percent coverage considering the area covered by each nucleosome. Lines show only the direct probe region, for which the percent occupancy for all positions that contribute to coverage is known. The locations of restriction sites used for the mapping are shown. The core 5S positioning sequence is indicated by a barbell on the bottom.

mononucleosome, altosome or dinucleosome fragments were calculated by comparison to the digestion control lanes using FluorChem 8800 software (GE Healthcare Life Sciences, USA). The signal from the larger of each pair of bands in a lane (>73 bp for mononucleosomes, >110 bp for altosomes and >146 bp for dinucleosomes) was multiplied by the length of the nucleosome species being probed and divided by the length of the larger

fragment. This calculation corrected for the intensity of the smaller band, simplifying the analysis. The percentage of each nucleosomal species present in the probe region (mononucleosome, altosome or dinucleosome) that was cut by each restriction enzyme to give a specific size fragment was then calculated by dividing this corrected intensity by the signal for the entire lane ('raw percent cutting'). The length and intensity of bands resulting from digestion at adjacent restriction sites was then used to map individual positions, with the 'percent cutting' for a given position calculated as the average raw percent cutting for all restriction digest bands resulting from that position. By comparing repeat experiments, the accuracy for assigning positions was calculated to be ±5 bp for mononucleosomes, ±7 bp for altosomes and ±9 bp for dinucleosomes.

Quantitation of nucleosome abundance in each probe region

Unlike our prior studies using minicircle templates containing only one nucleosome, more than one nucleosome may be present, on average, in the probed region on our polynucleosomal templates. The presence of multiple nucleosomes can decrease the percent cutting (and thus apparent occupancy) at any one position. For instance, if a region contained two perfectly positioned nucleosomes, digestion at a site covered by the first nucleosome would only result in 50% cutting, because that restriction enzyme will not cut fragments protected by the second nucleosome. To determine the total number of nucleosomes within each probe region, we compared the Southern signal for a given amount of bare template DNA digested with restriction enzymes (where no DNA is lost due to the digestion) to an equal amount of chromatin template that was digested with MNase (where linker DNA is eliminated). The ratio of signals for MNase-treated chromatin over restriction digested bare DNA tells the fraction of total DNA sequence in the probe region that is resistant to MNase digestion due to the presence of nucleosomes. When multiplied by the length of the probed region, this ratio establishes how many base pairs of DNA are covered by nucleosomes. Dividing this number by the 146-bp length of a single nucleosome gives the average number of nucleosomal units, present in any form, including mononucleosomes, altosomes or dinucleosomes, that cover the probed region. Note that the MNase digestion conditions required to map positions remove all linker DNA, but can also result in modest overdigestion of nucleosome-protected DNA (as indicated by the presence of some subnucleosomal DNA below the mononucleosomal band in Figure 1B, lane 1). Accordingly, the number of nucleosomes calculated by this method is likely to be slightly below the actual number in the probe region. Because of the high efficiency of nucleosome assembly over the 601 NPS, we were able to use an alternative method to calculate the number of nucleosomes in the probed region. Briefly, p601 chromatin was digested with BsiWI or with PmlI, both of which have unique sites (present only once in the whole plasmid) that are located within the 601 NPS. For both enzymes, cutting was ~6%, indicating that nucleosomes covered the NPS on 94% of all templates. We next multiplied the raw percent BsiWI cutting values for all mapped mononucleosomes, altosomes and dinucleosomes by the percentage of MNase products of mono-, alto- or dinucleosome size. The sum of these values was 75%, which is the fraction of all mapped MNase-resistant products that contain the BsiWI site. Since this is less than 94%, it indicates that there must be additional nucleosomes that overlap with the probe but not with the BsiWI site. More precisely, the ratio of 94%/75% tells the number of nucleosomes in the probe region, which in this case is 1.25. Note that this approach could not be used on the other templates due to the lack of restriction sites present in areas of high nucleosome occupancy that were also unique throughout the plasmid.

Calculation of percent occupancy

Mononucleosomes, dinucleosomes and altosomes can all exist on polynucleosomal templates, and make separate contributions to overall occupancy. Thus, to determine the fraction of templates containing a mononucleosome in any one position, we must multiply the percent cutting value by the fraction of all MNase-resistant products that are mononucleosomes. This number is determined from the MNase-digestion lanes (e.g. Figure 1B, lanes 1 and 5), by dividing the signal for the mononucleosome band by the signal for the entire lane. Incorporating all information about percent cutting, number of nucleosomes and percentage of each type of nucleosomal species gives the following equation: 'percent occupancy' = (percent cutting from restriction-digestion Southern gels) × (no. of nucleosomes in the region) × (percentage of MNase products of that size). For altosomes and dinucleosomes, this value was divided by 2, because these species contain two histone octamers. A step-by-step example of this method, applied to a model case, is presented in Supplementary Figure S1. Percent occupancy indicates the percentage of all templates that bear a mononucleosome, altosome or dinucleosome in each mapped position. By comparing duplicate + SWI/SNF and –SWI/SNF experiments on the same template, we calculated that the error in assigning percent occupancy was ±0.4% for individual mononucleosome positions and ±0.2% for individual altosome or dinucleosome positions.

RESULTS

To understand the effects of sequence on hSWI/SNF remodeling, we applied a novel chromatin mapping assay to four polynucleosomal templates containing promoter sequences from the 5S rDNA, c-myc and UGT1A1 genes, as well as the strong, artificial 601 positioning sequence. We began our analysis with a polynucleosomal template containing promoter sequences from the *Xenopus* somatic 5S rDNA. This is the same plasmid that was used to generate a mononucleosome minicircle template in our prior studies, which showed hSWI/SNF-directed movement of nucleosomes away from the well-characterized 5S positioning sequence (5S NPS) (29). These new experiments allow us to compare the effects of hSWI/SNF on the same sequence, but now in a polynucleosomal context.

The 5S rDNA plasmid was assembled into polynucleosomes by salt dilution (30), and remodeled with hSWI/SNF under conditions previously established to allow complete remodeling to a final hSWI/SNF-preferred chromatin state (22,29,30). Control and remodeled templates were digested with micrococcal nuclease (MNase), to remove all free DNA between nucleosomes, and MNase-resistant DNA fragments purified away from histones. On the unremodeled template, most fragments correspond to DNA covered by mononucleosomes and are ~146 bp in length (Figure 1B, lane 1, 'Mononuc'). However, there are also some ~292 bp fragments that correspond to the DNA protected when two nucleosomes are too close together for MNase to digest between them (Figure 1B, lane 1, 'Dinuc'). In addition, consistent with our prior studies, treatment with hSWI/SNF and ATP results in a great reduction of mononucleosome fragments and an increase in ~220-bp fragments characteristic of altosomes (Figure 1B, lane 5). To map the positions of mononucleosomes before and after hSWI/SNF remodeling, the ~146 bp mononucleosome products were isolated (Figure 1B, lanes 2 and 6). These fragments were then subjected to restriction enzyme digestion using enzymes with locally unique sites spaced ~50 bp apart throughout the 5S rDNA promoter region. These digestion products were then separated by PAGE and Southern blotted using a 359-bp probe spanning the 5S promoter region.

The Southern blot results for mononucleosomes from the control and remodeled 5S template are shown in Figure 1C. In this approach, any MNase-protected mononucleosomal fragment that contains a specific restriction site will be cut by that enzyme, yielding fragments whose lengths indicate individual nucleosome locations and whose intensities indicate individual nucleosome abundance (Figure 1A). While similar to the method we used previously to map nucleosome positions on mononucleosomal minicircles, this method also incorporates several novel analysis techniques that allow it to be applied to polynucleosomes (see 'Materials and methods' section and Supplementary Figure S1 for details). Briefly, by comparing the bands generated by adjacent restriction sites, mononucleosome positions can be mapped at a resolution of approximately ± 5 bp. For instance, the 116-bp ApaI and 110-bp EcoRV bands for the nonremodeled template (Figure 1C, left panel), correspond to an assembly favored mononucleosome position centered at +0 relative to the 5S transcription start site. To determine abundance, we calculated the percentage of bands in each lane corresponding to any given nucleosome position, and adjusted for the total number of nucleosomes present in the probed region, as well as for the fraction of these nucleosomes that were well-separated mononucleosomes. The resulting 'percent occupancy' value indicates the percentage of all templates that have a mononucleosome in each specific position. For the nonremodeled mononucleosome position indicated by the 116-bp ApaI and 110-bp EcoRV fragments, the final calculation (26% cutting × 1.85 nucleosomes in the region × 48% mononucleosomal) shows that chromatin assembly places a well-separated mononucleosome in this location on 23% of 5S templates (gray bar at approximately +0 in Figure 1D). This strong assembly-favored position is localized at the center of the 5S NPS, as mapped in prior studies by us and others (barbell in Figure 1D; 29,31,37).

The percent occupancy information for all detectable mononucleosome positions on the nonremodeled 5S template is shown as gray bars in Figure 1D (− SWI/SNF). Note that, in addition to a major position centered at +0 relative to the 5S transcription start site, there were also moderately strong satellite positions to either side. The presence of multiple overlapping preferred positions, which together result in a high combined occupancy over the center of the NPS, is characteristic of sequences containing the *Xenopus* 5S NPS (37). The positions seen for the center of the probed region also corresponded well with those seen when a single nucleosome was assembled onto the linear probe DNA fragment (29), indicating that the presence of neighboring nucleosomes did not prevent nucleosome formation on positions favored by the 5S NPS.

Notably, hSWI/SNF remodeling results in a 2- to 3-fold decrease in occupancy of all mononucleosomes at or near the 5S positioning sequence (Figure 1D, black bars). In addition, we also observed an hSWI/SNF-dependent increase in nucleosome occupancy at two upstream sequences after remodeling (at −131 and −73). Importantly, the polynucleosome templates were treated with SWI/SNF and ATP under conditions that allow SWI/SNF-driven repositioning and other remodeling effects to reach a dynamic equilibrium, at which continued remodeling does not result in any additional net change in nucleosome distribution (22,29,30). Thus, these positions represent the locations to which hSWI/SNF intrinsically prefers to place nucleosomes. These observations support the general conclusion from the minicircle studies that hSWI/SNF removes nucleosomes from strong NPSs and relocates them to hSWI/SNF-preferred sequences.

Even with maximum remodeling, however, we did not see the almost full removal of nucleosomes from the 5S NPS that was seen on minicircles. This suggests that, on polynucleosomal templates, the presence of neighboring nucleosomes might significantly constrain nucleosome repositioning, such that not all octamers can be moved away from NPSs. Interestingly, downstream of the 5S positioning sequence, there are four mononucleosome positions that show no significant change in occupancy after hSWI/SNF remodeling. Considering the significant change in occupancy over the positioning sequence, it is striking that this ~150-bp region very close to the positioning sequence shows no change as a result of SWI/SNF activity. As discussed further below, this may indicate that, in the context of adjacent nucleosomes on a polynucleosomal template, some positions may either resist remodeling or be equally favored by remodeling and assembly.

To get a sense of how control and remodeled mononucleosome positions contribute to the overall accessibility of DNA in chromatin, we assigned the percent occupancy for each nucleosome position to all sequences covered by that nucleosome (73-bp upstream and downstream from the center position), and summed these values for all mapped positions. When plotted versus DNA position,

this 'percent coverage' curve shows that the overlapping positions surrounding the major assembly preferred position together result in a high fraction of templates with a nucleosome covering the central part of the NPS (Figure 1D, gray line). They also show that hSWI/SNF remodeling greatly decreases DNA protection by mononucleosomes over the 5S positioning sequence (Figure 1D, black line).

hSWI/SNF moves nucleosomes away from a strong, artificial 601 positioning sequence

The results above indicate that hSWI/SNF moves nucleosomes away from strong NPSs on polynucleosomes. To more stringently test this hypothesis, we employed a plasmid containing the artificial, high-affinity 601 positioning sequence [one of the strongest known NPSs (34)]. When assembled into polynucleosomes, the 601 sequence forms mononucleosomes over the positioning sequence on over 80% of the templates assembled (Figure 2A). Compared to the natural 5S NPS, the 601 sequence has a considerably stronger positioning effect, such that only a single major position is observed, with no weaker positions formed directly to either side of the main position. However, downstream of the 601 NPS there are two weaker nucleosome positions, which add up to ~30% coverage, while the upstream sequences were entirely devoid of detectable mononucleosomes.

Remodeling of the 601 polynucleosome arrays by hSWI/SNF showed a dramatic movement away from the 601 NPS, reducing mononucleosome coverage of this region from ~80% to only ~15% (Figure 2A). This result further supports the conclusion that hSWI/SNF moves nucleosomes away from strong NPSs. It may also indicate that the stronger an NPS is, the greater the likelihood that hSWI/SNF will move nucleosomes away from it. As was also seen on the 5S template, reduction in mononucleosome coverage over the 601 NPS was accompanied by an increase in mononucleosomes on some hSWI/SNF-preferred sequences (four positions upstream of the NPS). Also as seen on 5S, there was one region where hSWI/SNF remodeling did not result in a great change in coverage (downstream of the NPS). These changes in mononucleosome positions were specifically due to ATP hydrolysis-dependent remodeling effects, since, in control experiments, 601 nucleosome occupancy was essentially unchanged when the template was incubated with hSWI/SNF in the absence of ATP (Supplementary Figure S2). Note that the apparent decrease in overall mononucleosome occupancy in the region is largely due to an increase in altosomes and dinucleosomes after hSWI/SNF remodeling—which will be addressed in detail in a later section.

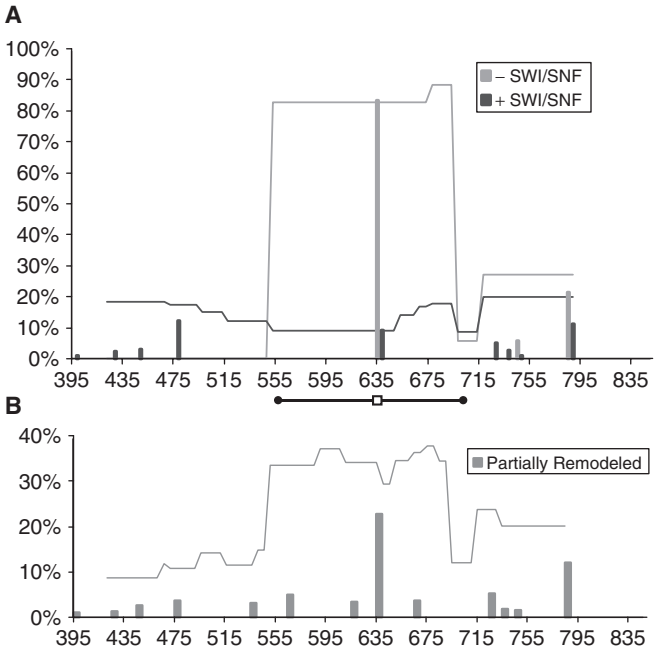

Figure 2. hSWI/SNF moves mononucleosomes away from the 601 high affinity positioning sequence on a polynucleosomal template. (**A**) Mononucleosome percent occupancy and % coverage for the 601 template either unremodeled (grey bars and lines) or fully remodeled (black bars and lines) are shown, as described for Figure 1D. (**B**) Mononucleosome percent occupancy and percent coverage on the partially remodeled 601 template (treated with hSWI/SNF for only 20 min) is shown as dark gray bars and lines.

Examining nucleosome positions after complete remodeling gives information about hSWI/SNF-favored nucleosome positions at equilibrium, but does not reveal possible intermediate steps in the remodeling reaction. To learn more about the process by which mononucleosomes are moved away from the 601 NPS, instead of 2.5 h, we allowed hSWI/SNF to act for only 20 min, and mapped the resulting positions. Partial remodeling on the 601 arrays resulted in the appearance of intermediate mononucleosome positions that overlapped with the 601 NPS (Figure 2B). When remodeling is complete, after 2.5 h, however, these intermediate positions are lost, together with an increase in hSWI/SNF-favored upstream positions (Figure 2A). This indicates that mononucleosome repositioning by hSWI/SNF does not result from large >100-bp jumps directly to favored positions, but proceeds in smaller steps, resulting in brief occupancy of sequences favored neither by assembly nor by hSWI/SNF.

Sequence-specific chromatin changes on human SWI/SNF target gene promoters

The 5S and 601 templates indicate the effects of strong, well-characterized, model NPSs on hSWI/SNF mononucleosome repositioning. To learn how sequence-directed remodeling effects might play a role in the transcriptional regulatory functions of hSWI/SNF, we next examined polynucleosomal templates containing promoter sequences from two known or suspected hSWI/SNF-regulated genes, c-myc and UGT1A1. hSWI/SNF activates c-myc expression in cycling cells, and was found to be associated with the c-myc promoter in cycling pre-B cells but not in resting, differentiated B cells (38, for review see 21). hSWI/SNF is also likely to be important for c-myc upregulation in response to estrogen, since it is an important coactivator for the estrogen receptor (39). Conversely, a subset of hSWI/SNF complexes (containing the variant ARID1A subunit) are also involved in c-myc

transcriptional repression (40, 41). Furthermore, two positioned nucleosomes at the proximal c-myc promoter (nucleosomes 12 and 13) appear to be 'disrupted' when c-myc transcription is activated, as assayed by indirect end labeling (32,33), and this chromatin change is potentially related to hSWI/SNF function in c-myc regulation. In our earlier studies, we found that the positions of nucleosomes 12 and 13 were recapitulated upon mononucleosome assembly onto minicircle templates, and that hSWI/SNF moved these mononucleosomes to locations away from positions 12 and 13 on the respective minicircles (29). To learn how hSWI/SNF action would change the nucleosomal arrangement on c-myc polynucleosomal chromatin, we used PCR from human genomic DNA to clone a ~2-kb region surrounding the major c-myc promoters P1 and P2, into a plasmid backbone. The chosen region encompasses nucleosomes 6–18 [using the numbering established by the Eick lab (32,33)]. We then mapped mononucleosome positions over the ~550-bp region surrounding nucleosomes 12 and 13. The unremodeled template displayed two clusters of nucleosome positions corresponding to the *in vivo* locations of 12 and 13 (Figure 3A, gray bars and lines), indicating that these sequences are functional NPSs. At both locations, we observed several mononucleosome positions that were staggered approximately every 10 bp, the periodicity

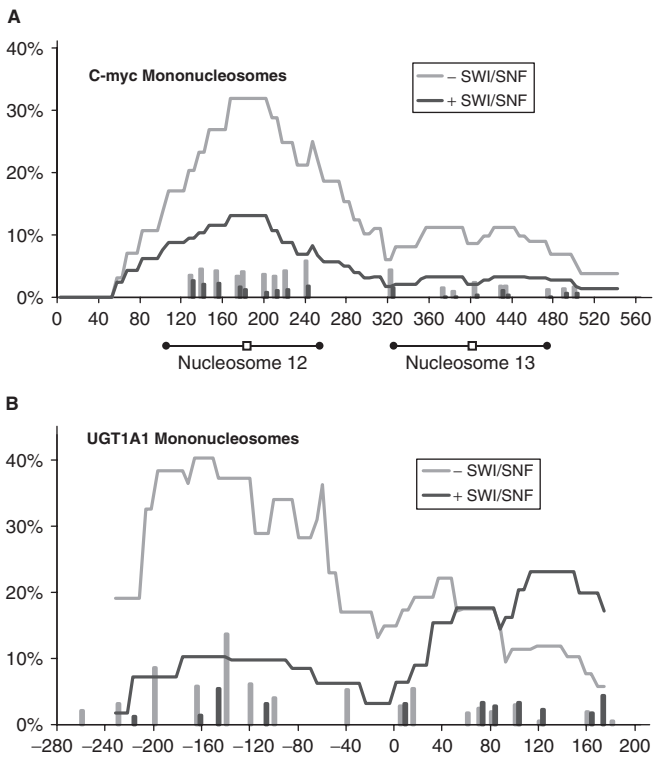

Figure 3. hSWI/SNF moves nucleosomes away from c-myc and UGT1A1 promoter positioning sequences. Mononucleosome percent occupancy and percent coverage from control (gray bars and lines) or remodeled (black bars and lines) c-myc polynucleosomes (**A**) and UGT1A1 polynucleosomes (**B**). The percent cutting values for the two c-myc probe regions were combined by equalizing the signals based on positions fully within the 179-bp overlap region of the two probes.

of the DNA wrapping around the nucleosome. Similar overlapping of preferred positions for 12 and 13 were also observed on unremodeled c-myc minicircles (29). This sort of clustering of mononucleosome positions around a single most-favored sequence is a common property of natural NPSs that appears to be intrinsic to their sequence characteristics (for review see 14).

The UGT1A1 gene encodes a drug-metabolizing enzyme essential for the break down of endogenous bilirubin as well as for the metabolism of drugs such as the chemotherapeutic agent irinotecan (for review see 42). UGT1A1 is also likely to be an hSWI/SNF target gene, since its transcription is activated by the glucocorticoid and aryl hydrocarbon receptors, both of which recruit SWI/SNF as a coactivator (43–46). When we mapped the nonremodeled mononucleosome positions on a polynucleosomal plasmid template containing 1 kb of human UGT1A1 promoter sequences, we found two peaks of nucleosome positions, a major one upstream of the transcription start site and a minor one downstream (Figure 3B, gray lines and bars). Again, the clustering of nucleosome positions with offsets in increments of ~10 or ~20 bp from peak favored positions, is typical of natural NPSs. No direct data exist regarding UGT1A1 promoter nucleosome positions *in vivo*. However, given the strong general correspondence between positions observed *in vivo* and positions favored by assembly *in vitro* [e.g. the results shown here for c-myc and for review see (14)], the assembly favored positions we observe here for UGT1A1 promoter polynucleosomes are likely to reflect NPSs that are relevant to UGT1A1 regulation *in vivo*.

hSWI/SNF remodeling of both the c-myc and the UGT1A1 templates resulted in a significant reduction of mononucleosomes at all positions that were strongly favored by nucleosome assembly (Figure 3A and B, black bars and lines). This is consistent with our prior observations on c-myc mononucleosome minicircles, and provides further evidence that hSWI/SNF action results in mononucleosome depletion from NPS sequences. In the case of UGT1A1, reduced nucleosome occupancy at assembly favored sites was accompanied by an overall 2-fold increase in occupancy downstream at approximately +80. Furthermore, after remodeling, this region shows higher mononucleosome occupancy than any other region covered by our probe. These results provide evidence that, on some templates at least, repositioning by hSWI/SNF can result in removal of mononucleosomes from NPSs together with accumulation of mononucleosomes at other, hSWI/SNF-preferred locations. In contrast, on the c-myc template hSWI/SNF caused a decrease in mononucleosome abundance at almost all assembly-favored positions without any appreciable increase at other locations within the ~550-bp region assayed. This differs from what we saw for c-myc minicircle mononucleosomes; where, hSWI/SNF action resulted in placement of repositioned nucleosomes over a few hSWI/SNF favored sequences (29). However, the minicircle experiments were done on templates containing only a single nucleosome, where there were no constraints imposed by neighboring nucleosomes, and where altosomes and dinucleosomes could not be formed as a

result of hSWI/SNF action. In the following section, we show how these polynucleosome-specific effects contribute to the overall hSWI/SNF-remodeled chromatin state on c-myc and our other templates.

Contributions of sequence-directed altosome and dinucleosome formation to the remodeled chromatin state

hSWI/SNF action resulted in a decrease of mononucleosome-sized MNase fragments on every template assayed (Figures 1–3). While hSWI/SNF did result in a modest reduction in overall nucleosome occupancy over some of the probed regions (from 1.85 to 1.82 for 5S; from 1.26 to 1.06 for 601; from 1.79 to 1.47 for c-myc and from 1.98 to 1.71 for UGT1A1), movement of nucleosomes out of the probe region could not explain the drop in mononucleosome abundance. For instance, hSWI/SNF causes total nucleosomes in the 601 template probed region to drop by 1.2-fold but causes mononucleosome abundance to drop by 1.8-fold. The additional decrease in mononucleosome abundance results from hSWI/SNF conversion of a large fraction of well-separated mononucleosomes into altosomes and dinucleosomes (e.g. Figure 1B, lane 1 versus lane 5). After remodeling, these nonmononucleosomal structures become a major fraction of total species. In Figure 1B, for example, MNase fragments larger than mononucleosome in length increase from 47% to 64%. Accordingly, a full understanding of the properties of hSWI/SNF-remodeled chromatin will require knowing about the localization and abundance of mononucleosomes as well as altosomes and dinucleosomes (which make up the bulk of nonmononucleosomal species).

Due to the different lengths of DNA covered by altosomes and dinucleosomes, as compared to mononucleosomes, no existing chromatin mapping approaches were expected to be effective for mapping these species. Indeed, the large footprints of these species could easily confound approaches such as indirect end labeling that assume a ~146-bp mononucleosomal footprint. The mapping strategy developed here, however, could be readily adapted to map and quantitate altosomes and dinucleosomes. To do so, we isolated ~220-bp altosomal and ~290-bp dinucleosomal fragments, as opposed to ~146-bp mononucleosomal fragments (Figure 1B, lanes 3, 4 and 7, 8). These were then restriction digested and mapped essentially as described for mononucleosomes. Note that, here and in previous studies, we never observed a discrete ~220-bp altosome footprint band after MNase digestion of nonremodeled templates [e.g. Figure 1B, lane 1 and (30)]. This led us to speculate that altosomes were only formed as a result of hSWI/SNF action, and that ~220-bp fragments from control samples arise from either MNase overdigestion of one or both ends of dinucleosomes or underdigestion of one or both ends of mononucleosomes. If this was the case, these fragments would lack discrete ends, which would preclude mapping of their positions. However, when we mapped the ~220-bp products from nonremodeled reactions, we saw that they localized to a few discrete positions (Figure 4A, C and D, gray bars). This suggests that altosomes can naturally form without SWI/SNF action. On the other hand, their low abundance indicates that their formation during chromatin assembly is either kinetically or energetically unfavorable. This is consistent with our prior observation that hSWI/SNF-generated altosomes are metastable structures that revert to normal mono- and dinucleosomes when incubated for several hours at 37°C after cessation of remodeling (30). hSWI/SNF can also connect two individual mononucleosomes (each on separate ~155-bp DNA fragments) together into altered dimers, which have many properties in common with altosomes (47). Altered dimers were also shown to form at low levels during salt dialysis assembly (48), suggesting that both structures are allowable, but unfavorable, products of assembly, whose formation is enhanced by hSWI/SNF action.

On all templates where altosomes were mapped under both + and –SWI/SNF conditions, remodeling caused an overall ~2- to 4-fold increase in altosome abundance (Figure 4A, C and D, top panels). Remodeling also resulted in a lesser increase in dinucleosome abundance on 5S and c-myc, as well as a decrease in dinucleosome abundance over the left half of the 601-probed region (Figure 4A, B and C, middle panels). In some cases, remodeling resulted in altosome and dinucleosome formation at hSWI/SNF-preferred sites, where these products were either not present or very weakly present after assembly. For instance, several new altosome and dinucleosome positions appear after remodeling on the downstream half of the 5S-probed region. In most other cases, hSWI/SNF tended to increase altosome and dinucleosome percent occupancy at sites where these species had been detectable after assembly. Finally, in a few cases, hSWI/SNF action decreased dinucleosome or altosome occupancy (e.g. Figure 4B, dinucleosome at position 575; and Figure 4C, altosome at position 455). Overall, these results indicate that altosomes and dinucleosomes are formed at specific positions during assembly, and that the level of these species can vary greatly between templates. They also show that hSWI/SNF action can both increase the abundance of these species and promote their formation at hSWI/SNF-preferred locations.

Because of their abundance (especially after hSWI/SNF remodeling), altosomes and dinucleosomes contribute significantly to the overall nucleosomal coverage of each template. The combined coverage curves for all measured species (mononucleosomes, altosomes and dinucleosomes) are shown in the lower panels in Figure 4 (solid lines indicate total coverage, dotted lines indicate mononucleosomes alone). Notably, the aggregate effect of hSWI/SNF differed greatly between templates. On the UGT1A1 template, hSWI/SNF caused a pronounced shift in coverage from upstream to downstream of the transcription start site. On 5S and 601, hSWI/SNF largely erased the effect of the NPS, promoting more even accessibility across the region. Importantly, this was the result of the total individual contributions of sequence-specific mononucleosome, altosome and dinucleosome positions, and was not because hSWI/SNF randomized all nucleosome positions evenly. Finally, at c-myc, the combined coverage of all products after hSWI/SNF was similar to that before hSWI/SNF. This is because when hSWI/SNF converted

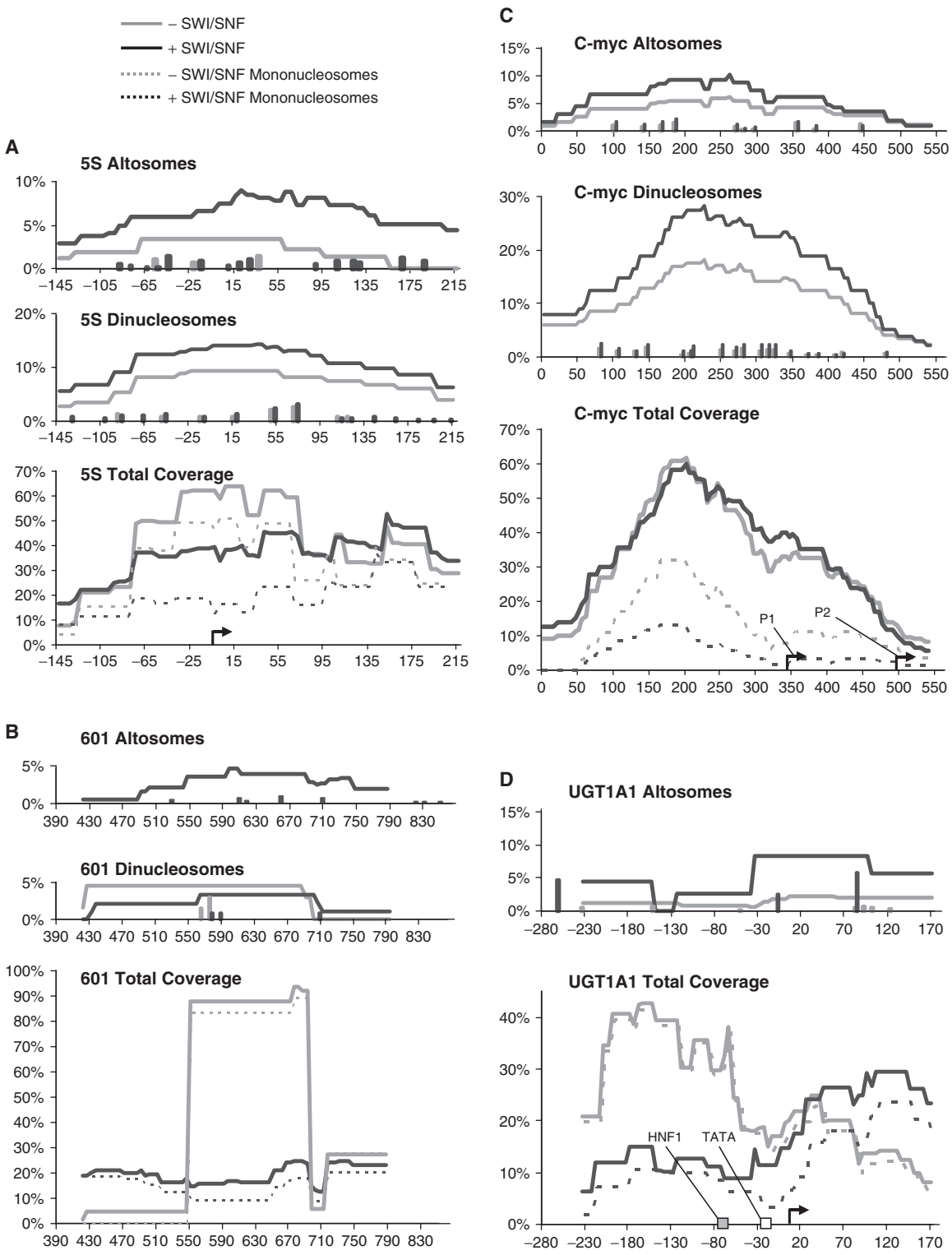

Figure 4. hSWI/SNF increases the number of altosomes and dinucleosomes at specific locations on the 5S, 601, c-myc and UGT1A1 templates. Bars show the percent occupancy for centers of individual altosome (top graphs) or dinucleosome positions (middle graphs, where this data were available) for 5S (**A**), 601 (**B**), c-myc (**C**) and UGT1A1 (**D**). Lines show the percent coverage for each species given a 220-bp footprint size for altosomes and a 292-bp footprint size for dinucleosomes. Gray bars and lines represent unremodeled templates, while black bars and lines represent remodeled templates. The lower graphs show overall coverage summed for all mapped mononucleosome, altosome and dinucleosomes positions on control (gray lines) or remodeled (black lines) templates. For reference, dotted lines show the percent mononucleosome coverage curves (from Figures 1, 2 and 3). The positions of the HNF1 site and putative TATA box on UGT1A1 and all relevant transcription start sites are indicated.

mononucleosomes to altosomes and dinucleosomes on this sequence, their placement happened to result in relatively little change in overall nucleosome coverage. However, as we will discuss later, even though there is no dramatic change in overall nucleosome coverage, the conversion of mononucleosomes to other species could potentially alter the availability of promoter sequences to transcription factors.

Characteristics of altosome and dinucleosome positions

We noticed that many restriction digestion bands from altosomes and dinucleosomes had the exact same gel mobility as bands from mononucleosome fragments digested with the same restriction enzymes (arrows in Figure 5A). This indicated that mononucleosomes, altosomes and dinucleosomes might frequently have one edge in common, resulting in an identical fragment length when these ~146-, ~220- and ~290-bp MNase products were digested with a restriction enzyme near that edge. After mapping all altosome and dinucleosome positions for all four hSWI/SNF remodeled templates, we found that 31 out of 41 altosome positions and 29 out of 36 dinucleosome positions shared either a left or right edge (within 5 bp) of a nonremodeled mononucleosome position. We next calculated the chance that a randomly positioned altosome or dinucleosome would have an edge located ± 5 bp from an assembly-favored mononucleosome edge, and used this to determine the probability that the observed distribution would occur by random chance. For both altosomes and dinucleosomes, the calculated *P*-values were <0.0001. These results indicate that altosomes and dinucleosomes contain one histone octamer in an assembly-favored position, suggesting that these species are formed when a mononucleosome being moved by hSWI/SNF encounters an unmoved nucleosome.

DISCUSSION

Our results indicate that hSWI/SNF has two major effects on polynucleosomal templates: mononucleosome repositioning away from NPSs and formation of altosomes and dinucleosomes at specific locations (as illustrated in Figure 5B–E). First, consistent with our findings on mononucleosomal minicircles, hSWI/SNF moves nucleosomes away from strong NPSs (thick gray lines), which can result in increased mononucleosome abundance at specific hSWI/SNF-preferred positions (thick black lines, Figure 5B–E, nucleosome 2). Current models argue that repositioning occurs when a remodeling complex pulls DNA into a nucleosome, creating a loop or bulge of DNA. When this loop moves around the surface of the octamer and is released from the far edge, this results in movement of the nucleosome by the length of the loop [Figure 5C–E, nucleosome 2 (49,50)]. Interestingly, our analysis of the partially remodeled 601 template indicates that repositioning from NPSs to hSWI/SNF-preferred positions does not occur all at once, but proceeds through intermediate positions that are as little as ~20 bp away, and that are not favored by assembly or by complete remodeling. These intermediate sites might potentially be weak NPSs, which are not occupied after assembly because the 601 NPS is predominant and suppresses formation of nucleosomes at any overlapping positions. In the framework of the loop model for repositioning, the distances that we observe between intermediate

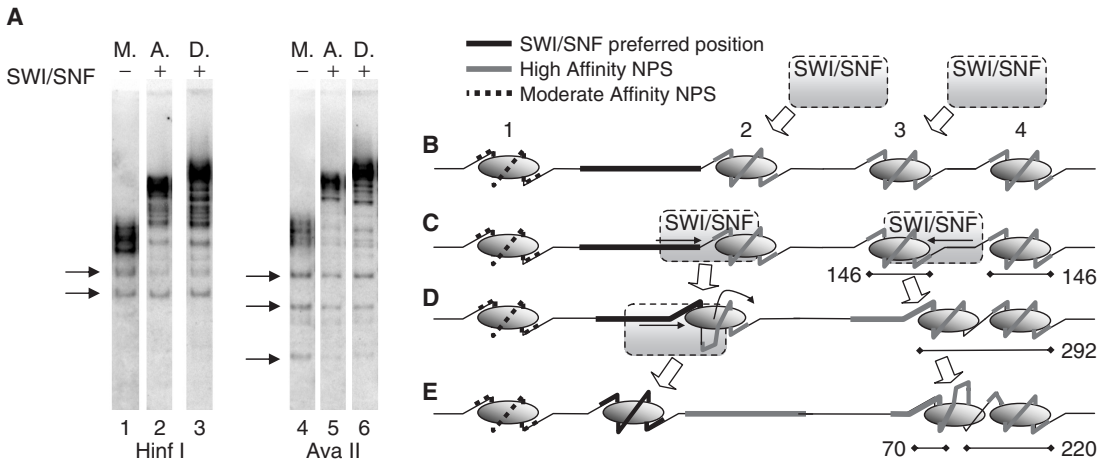

Figure 5. Altosomes and dinucleosomes appear to form when an hSWI/SNF repositioned nucleosome encounters an unmoved nucleosome. (**A**) Comparison of HinfI and AvaII restriction digestion lanes of mononucleosomal MNase fragments for the unremodeled c-myc template ('M.', hSWI/SNF) and altosomes ('A.') or dinucleosomes ('D.') for the hSWI/SNF-remodeled c-myc template (+SWI/SNF). Arrows indicate digestion products that are exactly the same length for all three nucleosome species. (**B–E**) Model for hSWI/SNF-remodeling effects on four nucleosomes (1–4). The '1' represents a nucleosome located on a moderately strong NPS (dotted line) whose occupancy does not change as a result of remodeling; '2' represents a nucleosome on one strong NPS (B-2, gray line). hSWI/SNF moves it way from the NPS, passing through repositioning intermediates that likely involve formation and resolution of a DNA loop on the surface of the octamer (D-2), to an equilibrium remodeled position on an hSWI/SNF favored sequence (E-2, black line). The '3' represents a nucleosome on an NPS which has no nearby hSWI/SNF-favored sequence to move to. hSWI/SNF may move this nucleosome into an unmoved nucleosome to create a normal dinucleosome (D-3 and -4) or an altosome (E-3 and -4). Bars under nucleosomes 3 and 4 show the resulting MNase footprint sizes.

remodeling positions suggest that the step size for repositioning (and thus the length of the loop) can be between ~20 bp and ~60 bp. We also found that nucleosomes in some positions that are less favored by assembly (thick striped lines) appear to either not be moved by hSWI/SNF or, if they are moved, are equally preferred by hSWI/SNF and by assembly (Figure 5B, nucleosome 1).

While we do not yet know the detailed properties of the DNA sequences to which hSWI/SNF prefers to move nucleosomes, our recent studies offer a few initial hints. First, on both polynucleosomes and minicircles, we found that hSWI/SNF rarely caused mononucleosomes to adopt new positions that were completely absent from the non-remodeled chromatin template [this study and (29)]. We also found that well-separated mononucleosomes resulting from hSWI/SNF action are structurally normal (30). These observations imply that movement of a nucleosome by SWI/SNF must still be to sequences that can facilitate proper wrapping of the DNA around the histone octamer, and not to sequences on which it is thermodynamically impractical to assemble a nucleosome. Theoretically, the repositioning specificity we observe here could arise from sequence preferences of hSWI/SNF subunits at different stages of the remodeling reaction. For instance, a DNA-binding subunit that has a particularly strong affinity for a given sequence might cause the remodeling complex to pause, creating a favored position. Alternatively, strong binding affinity may aid the complex in productively engaging with a given nucleosome, promoting movement either toward or away from this sequence. In constrast, we do not think that the sequence specificity of hSWI/SNF remodeling results from passive effects, such as one hSWI/SNF complex binding to a specific site and acting as a steric barrier to a nucleosome being moved by another hSWI/SNF complex. This is suggested by our prior observations that changes in stable restriction enzyme accessibility suggestive of repositioning away from NPSs could be seen at hSWI/SNF : nucleosome ratios ranging from ~3:1 to 0.1:1 (30,35), and also by the relatively low measured affinity of the hSWI/SNF ATPase, BRG1, for nucleosomes (51). In addition, in the presence of ATP, hSWI/SNF is expected to continue moving along DNA and repositioning nucleosomes, such that it will not remain in any one place for long enough to have a steric effect. Note that the intrinsic sequence specificity of hSWI/SNF remodeling may be modulated *in vivo* by other factors present on promoter chromatin, such that the final remodeled chromatin state may result from a combination of DNA sequence, hSWI/SNF, transcription factors, histone tail modifications and/or other chromatin proteins, such as linker histones, HMGs or HP1.

In addition to mononucleosome repositioning away from NPSs, hSWI/SNF also promotes the formation of altosomes and normal dinucleosomes. These products can account for a large fraction of remodeled nucleosomes, indicating that approaches that only examine mononucleosome positions will reveal only a partial picture of the chromatin landscape at hSWI/SNF-regulated genes. The observation that altosomes and dinucleosomes frequently have one edge in common with a nonremodeled mononucleosome suggests that these products form when a nucleosome being repositioned by hSWI/SNF collides with a second, unmoved mononucleosome present on an NPS. If the repositioning reaction stops such that both nucleosomes are structurally normal, this would result in a dinucleosome with one edge established by the location of the nonmoved mononucleosome (Figure 5D, nucleosomes 3 and 4, with MNase footprint sizes indicated by barbells). Alternatively, a collision with an unmoved nucleosome might prevent the resolution of the DNA loop that is thought to be required for repositioning. If so, this would result in an altosome that after MNase digestion would give a ~220-bp product with one edge the same as an edge of the un-moved mononucleosome and the other edge being the position of the MNase accessible loop of DNA (Figure 5E, nucleosomes 3 and 4). In our prior studies, we showed that altosomes were also associated with a second ~70-bp fragment. Because of their small size, we were not able to use our mapping approach to determine the location of these fragments. However, from the known characteristics of altosomes, together with the mapped positions of the ~220-bp altosome footprint fragments, we expect that these fragments will be localized away from the un-moved nucleosome at the other side of the putative loop (Figure 5E, nucleosomes 3 and 4, barbell marked '70').

The balance between mononucleosome repositioning and altosome/dinucleosome formation might potentially be controlled by a combination of local nucleosome density and hSWI/SNF preference. For instance, if there were no desirable sequences to move mononucleosomes to within a window of ~100 bp, collisions with nonmoved nucleosomes would tend to happen before a favored site is found, and remodeling would tend to favor altosome and dinucleosome formation (e.g. Figure 5C–E, nucleosome 3 versus nucleosome 2). This might be the case, for instance, on the c-myc promoter, where hSWI/SNF remodeling gives no complex-favored mononucleosome positions, but results in the greatest increase in altosomes and dinucleosomes. Note that the *in vivo* presence of nucleosomes 12 and 13 on the inactive c-myc promoter was shown by an indirect end-labeling approach that can only identify a nucleosome position if an ~146-bp MNase insensitive region is surrounded by MNase sensitive sites (32,33). It is expected that the larger footprints of altosomes and dinucleosomes would confound this analysis and make it appear that these nucleosomes had been 'disrupted'. Thus, our observation that more than three quarters of the mapped nucleosomal species in this region after hSWI/SNF remodeling are altosomes and dinucleosomes may provide an explanation for the apparent disruption of these nucleosomes upon c-myc activation.

The sequence-specific chromatin remodeling effects we observe here could have important effects on transcription. For instance, on the UGT1A1 promoter, hSWI/SNF action decreased overall nucleosome coverage over the important HNF1 transcription factor binding site (44,52) by ~3-fold (Figure 4D). Second, while hSWI/SNF decreased overall coverage over the putative TATA box and transcription start site by only ~1.5-fold, altosomes became more abundant than mononucleosomes

at these positions. While altosomes inhibit the access of MNase to DNA to approximately the same extent as normal dinucleosomes [~220- plus ~70-bp altosomal versus ~290-bp dinucleosomal footprint sizes (30)], other results indicate that altosomes may be functionally distinct from normal nucleosomes. First, our recent studies showed that altered mononucleosome dimers (and by extension altosomes) have an inverted accessibility profile for transcription factors (47). In addition, DNA accessibility to nucleosome-covered sequences is greatest at sites where DNA enters or leaves the histone octamer (53,54). Thus, by providing two additional entry points, the accessible loop on the altosome might greatly increase the ability of transcription factors to bind at nearby sites. Altosomes can also revert over time to normal nucleosomes (30), and this suggests that they are high-energy structures which may be more easily invaded by transcription factors. Conversely, transcription factors that attempt to bind to sites covered by altosomes could potentially promote reversion, and may also influence the placement of the resulting normal nucleosomes.

In conclusion, recent studies showing that the nucleosomes are frequently positioned *in vivo* have suggested that promoters are evolutionarily selected to encode both consensus sites for transcription factors and default assembly-favored NPSs (3–13, and for review see 14). The relative arrangement of these NPSs may then either allow or inhibit transcription. Our results extend this model, indicating that an intrinsic preference to move nucleosomes off of NPSs gives hSWI/SNF the potential to automatically switch promoter chromatin away from a default NPS-specified state. This provides a potential mechanism by which hSWI/SNF can have opposing effects when recruited to different sequences. For instance, hSWI/SNF- and sequence-directed movement away from an NPS might just as easily repress transcription if it opened up binding sites for transcriptional repressors, or created a new peak of coverage over activator or basal factor binding sites. Intriguingly, the observation that hSWI/SNF moves mononucleosomes to complex-favored positions and forms specifically positioned altosomes and dinucleosomes suggests that hSWI/SNF-regulated promoters may be evolutionarily selected not only for default NPSs, but also for sequences that direct the proper active or repressive hSWI/SNF-remodeled chromatin states. Finally, given the core conservation of all ATP-dependent remodeling subunits, these results indicate that the effects of other remodeling complexes may also be controlled by DNA sequence. If so, recruitment of different remodeling complexes might result in a variety of, potentially opposing, remodeled-chromatin arrangements.

SUPPLEMENTARY DATA

Supplementary Data are available at NAR Online.

ACKNOWLEDGEMENTS

The authors would like to thank Dr Michael Court for the UGT1A1 promoter plasmid, Anastasie Kweudju for help with some polynucleosomal template assemblies and Drs A. Imbalzano and G. Narlikar for critical reading of the article.

FUNDING

National Institutes of Health (DK079300 to G.R.S.); The American Cancer Society (RSG-04-188 to G.R.S.). Funding for open access charge: ACS RSG-04-188.

Conflict of interest statement. None declared.

REFERENCES

1. Wolffe,A.P. (2001) Transcriptional regulation in the context of chromatin structure. *Essays Biochem.*, **37**, 45–57.
2. Zhang,H. and Reese,J.C. (2007) Exposing the core promoter is sufficient to activate transcription and alter coactivator requirement at RNR3. *Proc. Natl Acad. Sci. USA*, **104**, 8833–8838.
3. Ioshikhes,I.P., Albert,I., Zanton,S.J. and Pugh,B.F. (2006) Nucleosome positions predicted through comparative genomics. *Nat. Genet.*, **38**, 1210–1215.
4. Segal,E., Fondufe-Mittendorf,Y., Chen,L., Thastrom,A., Field,Y., Moore,I.K., Wang,J.P. and Widom,J. (2006) A genomic code for nucleosome positioning. *Nature*, **442**, 772–778.
5. Yuan,G.C., Liu,Y.J., Dion,M.F., Slack,M.D., Wu,L.F., Altschuler,S.J. and Rando,O.J. (2005) Genome-scale identification of nucleosome positions in S. cerevisiae. *Science*, **309**, 626–630.
6. Albert,I., Mavrich,T.N., Tomsho,L.P., Qi,J., Zanton,S.J., Schuster,S.C. and Pugh,B.F. (2007) Translational and rotational settings of H2A.Z nucleosomes across the Saccharomyces cerevisiae genome. *Nature*, **446**, 572–576.
7. Peckham,H.E., Thurman,R.E., Fu,Y., Stamatoyannopoulos,J.A., Noble,W.S., Struhl,K. and Weng,Z. (2007) Nucleosome positioning signals in genomic DNA. *Genome Res.*, **17**, 1170–1177.
8. Lee,W., Tillo,D., Bray,N., Morse,R.H., Davis,R.W., Hughes,T.R. and Nislow,C. (2007) A high-resolution atlas of nucleosome occupancy in yeast. *Nat. Genet.*, **39**, 1235–1244.
9. Miele,V., Vaillant,C., d'Aubenton-Carafa,Y., Thermes,C. and Grange,T. (2008) DNA physical properties determine nucleosome occupancy from yeast to fly. *Nucleic Acids Res.*, **36**, 3746–3756.
10. Shivaswamy,S., Bhinge,A., Zhao,Y., Jones,S., Hirst,M. and Iyer,V.R. (2008) Dynamic remodeling of individual nucleosomes across a eukaryotic genome in response to transcriptional perturbation. *PLoS Biol.*, **6**, e65.
11. Schones,D.E., Cui,K., Cuddapah,S., Roh,T.Y., Barski,A., Wang,Z., Wei,G. and Zhao,K. (2008) Dynamic regulation of nucleosome positioning in the human genome. *Cell*, **132**, 887–898.
12. Ozsolak,F., Song,J.S., Liu,X.S. and Fisher,D.E. (2007) High-throughput mapping of the chromatin structure of human promoters. *Nat. Biotechnol.*, **25**, 244–248.
13. Johnson,S.M., Tan,F.J., McCullough,H.L., Riordan,D.P. and Fire,A.Z. (2006) Flexibility and constraint in the nucleosome core landscape of Caenorhabditis elegans chromatin. *Genome Res.*, **16**, 1505–1516.
14. Schnitzler,G.R. (2008) Control of nucleosome positions by DNA sequence and remodeling machines. *Cell Biochem. Biophys.*, **51**, 67–80.
15. Narlikar,L., Gordan,R. and Hartemink,A.J. (2007) A nucleosome-guided map of transcription factor binding sites in yeast. *PLoS Comput. Biol.*, **3**, e215.
16. Ramachandran,A. and Schnitzler,G. (2004) Regulating transcription one nucleosome at a time: nature and function of chromatin remodeling complex products. *Recent Res. Devel. Mol. Cell Biol.*, **5**, 149–170.
17. Saha,A., Wittmeyer,J. and Cairns,B.R. (2006) Chromatin remodelling: the industrial revolution of DNA around histones. *Nat. Rev. Mol. Cell Biol.*, **7**, 437–447.
18. de la Serna,I.L., Ohkawa,Y. and Imbalzano,A.N. (2006) Chromatin remodelling in mammalian differentiation: lessons from ATP-dependent remodellers. *Nat. Rev. Genet.*, **7**, 461–473.

19. Chen,J., Kinyamu,H.K. and Archer,T.K. (2006) Changes in attitude, changes in latitude: nuclear receptors remodeling chromatin to regulate transcription. *Mol. Endocrinol.*, **20**, 1–13.
20. Simone,C. (2005) SWI/SNF: the crossroads where extracellular signaling pathways meet chromatin. *J. Cell Physiol.*, **207**, 309–314.
21. Klochendler-Yeivin,A., Muchardt,C. and Yaniv,M. (2002) SWI/SNF chromatin remodeling and cancer. *Curr. Opin. Genet. Dev.*, **12**, 73–79.
22. Ramachandran,A., Omar,M., Cheslock,P. and Schnitzler,G.R. (2003) Linker histone H1 modulates nucleosome remodeling by human SWI/SNF. *J. Biol. Chem.*, **278**, 48590–48601.
23. Kassabov,S.R., Zhang,B., Persinger,J. and Bartholomew,B. (2003) SWI/SNF unwraps, slides, and rewraps the nucleosome. *Mol. Cell*, **11**, 391–403.
24. Aoyagi,S., Narlikar,G., Zheng,C., Sif,S., Kingston,R.E. and Hayes,J.J. (2002) Nucleosome remodeling by the human SWI/SNF complex requires transient global disruption of histone-DNA interactions. *Mol. Cell Biol.*, **22**, 3653–3662.
25. Fan,H.Y., He,X., Kingston,R.E. and Narlikar,G.J. (2003) Distinct strategies to make nucleosomal DNA accessible. *Mol. Cell*, **11**, 1311–1322.
26. Bruno,M., Flaus,A., Stockdale,C., Rencurel,C., Ferreira,H. and Owen-Hughes,T. (2003) Histone H2A/H2B dimer exchange by ATP-dependent chromatin remodeling activities. *Mol. Cell*, **12**, 1599–1606.
27. Gutierrez,J., Paredes,R., Cruzat,F., Hill,D.A., van Wijnen,A.J., Lian,J.B., Stein,G.S., Stein,J.L., Imbalzano,A.N. and Montecino,M. (2007) Chromatin remodeling by SWI/SNF results in nucleosome mobilization to preferential positions in the rat osteocalcin gene promoter. *J. Biol. Chem.*, **282**, 9445–9457.
28. Rippe,K., Schrader,A., Riede,P., Strohner,R., Lehmann,E. and Langst,G. (2007) DNA sequence- and conformation-directed positioning of nucleosomes by chromatin-remodeling complexes. *Proc. Natl Acad. Sci. USA*, **104**, 15635–15640.
29. Sims,H.I., Lane,J.M., Ulyanova,N.P. and Schnitzler,G.R. (2007) Human SWI/SNF drives sequence-directed repositioning of nucleosomes on C-myc promoter DNA minicircles. *Biochemistry*, **46**, 11377–11388.
30. Ulyanova,N.P. and Schnitzler,G.R. (2005) Human SWI/SNF generates abundant, structurally altered dinucleosomes on polynucleosomal templates. *Mol. Cell Biol.*, **25**, 11156–11170.
31. Hayes,J.J. and Wolffe,A.P. (1992) Histones H2A/H2B inhibit the interaction of transcription factor IIIA with the Xenopus borealis somatic 5S RNA gene in a nucleosome. *Proc. Natl Acad. Sci. USA*, **89**, 1229–1233.
32. Albert,T., Wells,J., Funk,J.O., Pullner,A., Raschke,E.E., Stelzer,G., Meisterernst,M., Farnham,P.J. and Eick,D. (2001) The chromatin structure of the dual c-myc promoter P1/P2 is regulated by separate elements. *J. Biol. Chem.*, **276**, 20482–20490.
33. Pullner,A., Mautner,J., Albert,T. and Eick,D. (1996) Nucleosomal structure of active and inactive c-myc genes. *J. Biol. Chem.*, **271**, 31452–31457.
34. Lowary,P.T. and Widom,J. (1998) New DNA sequence rules for high affinity binding to histone octamer and sequence-directed nucleosome positioning. *J. Mol. Biol.*, **276**, 19–42.
35. Schnitzler,G.R., Cheung,C.L., Hafner,J.H., Saurin,A.J., Kingston,R.E. and Lieber,C.M. (2001) Direct imaging of human SWI/SNF-remodeled mono- and polynucleosomes by atomic force microscopy employing carbon nanotube tips. *Mol. Cell Biol.*, **21**, 8504–8511.
36. Schnitzler,G., Sif,S. and Kingston,R.E. (1998) Human SWI/SNF interconverts a nucleosome between its base state and a stable remodeled state. *Cell*, **94**, 17–27.
37. Ura,K., Hayes,J.J. and Wolffe,A.P. (1995) A positive role for nucleosome mobility in the transcriptional activity of chromatin templates: restriction by linker histones. *EMBO J.*, **14**, 3752–3765.
38. Chi,T.H., Wan,M., Lee,P.P., Akashi,K., Metzger,D., Chambon,P., Wilson,C.B. and Crabtree,G.R. (2003) Sequential roles of Brg, the ATPase subunit of BAF chromatin remodeling complexes, in thymocyte development. *Immunity*, **19**, 169–182.
39. DiRenzo,J., Shang,Y., Phelan,M., Sif,S., Myers,M., Kingston,R. and Brown,M. (2000) BRG-1 is recruited to estrogen-responsive promoters and cooperates with factors involved in histone acetylation. *Mol. Cell Biol.*, **20**, 7541–7549.
40. Nagl,N.G. Jr, Zweitzig,D.R., Thimmapaya,B., Beck,G.R. Jr and Moran,E. (2006) The c-myc gene is a direct target of mammalian SWI/SNF-related complexes during differentiation-associated cell cycle arrest. *Cancer Res.*, **66**, 1289–1293.
41. Nagl,N.G. Jr, Wang,X., Patsialou,A., Van Scoy,M. and Moran,E. (2007) Distinct mammalian SWI/SNF chromatin remodeling complexes with opposing roles in cell-cycle control. *Embo. J.*, **26**, 752–763.
42. Guillemette,C. (2003) Pharmacogenomics of human UDP-glucuronosyltransferase enzymes. *Pharmacogenomics J.*, **3**, 136–158.
43. Wang,S. and Hankinson,O. (2002) Functional involvement of the BRM/SWI2-related gene 1 protein (BRG-1)in cytochrome P4501A1 transcription mediated by the aryl hydrocarbon receptor complex. *J. Biol. Chem.*, **277**, 11821–11827.
44. Sugatani,J., Mizushima,K., Osabe,M., Yamakawa,K., Kakizaki,S., Takagi,H., Mori,M., Ikari,A. and Miwa,M. (2008) Transcriptional regulation of human UGT1A1 gene expression through distal and proximal promoter motifs: implication of defects in the UGT1A1 gene promoter. *Naunyn Schmiedebergs Arch. Pharmacol.*, **377**, 597–605.
45. Fryer,C.J. and Archer,T.K. (1998) Chromatin remodelling by the glucocorticoid receptor requires the BRG1 complex. *Nature*, **393**, 88–91.
46. Sugatani,J., Nishitani,S., Yamakawa,K., Yoshinari,K., Sueyoshi,T., Negishi,M. and Miwa,M. (2005) Transcriptional regulation of human UGT1A1 gene expression: activated glucocorticoid receptor enhances constitutive androstane receptor/pregnane X receptor-mediated UDP-glucuronosyltransferase 1A1 regulation with glucocorticoid receptor-interacting protein 1. *Mol. Pharmacol.*, **67**, 845–855.
47. Ulyanova,N.P. and Schnitzler,G.R. (2006) Inverted factor access and slow reversion characterize SWI/SNF-altered nucleosome dimers. *J. Biol. Chem.*, **282**, 1018–1028.
48. Schnitzler,G.R., Sif,S. and Kingston,R.E. (1998) A model for chromatin remodeling by the SWI/SNF family. *Cold Spring Harb. Symp. Quant. Biol.*, **63**, 535–543.
49. Flaus,A. and Owen-Hughes,T. (2003) Mechanisms for nucleosome mobilization. *Biopolymers*, **68**, 563–578.
50. Cairns,B.R. (2007) Chromatin remodeling: insights and intrigue from single-molecule studies. *Nat. Struct. Mol. Biol.*, **14**, 989–996.
51. Narlikar,G.J., Phelan,M.L and Kingston,R.E. (2001) Generation and interconversion of multiple distinct nucleosomal states as a mechanism for catalyzing chromatin fluidity. *Mol. Cell*, **8**, 1219–1230.
52. Bernard,P., Goudonnet,H., Artur,Y., Desvergne,B. and Wahli,W. (1999) Activation of the mouse TATA-less and human TATA-containing UDP-glucuronosyltransferase 1A1 promoters by hepatocyte nuclear factor 1. *Mol. Pharmacol.*, **56**, 526–536.
53. Anderson,J.D., Thastrom,A. and Widom,J. (2002) Spontaneous access of proteins to buried nucleosomal DNA target sites occurs via a mechanism that is distinct from nucleosome translocation. *Mol. Cell Biol.*, **22**, 7147–7157.
54. Li,G. and Widom,J. (2004) Nucleosomes facilitate their own invasion. *Nat. Struct. Mol. Biol.*, **11**, 763–769.